THE JOURNAL OF PHYSICAL CHEMISTRY A

Article

pubs.acs.org/JPCA

Computational Study on the Effect of Hydration on New Particle Formation in the Sulfuric Acid/Ammonia and Sulfuric Acid/Dimethylamine Systems

Henning Henschel,*[,†] Theo Kurtén,[‡] and Hanna Vehkamäki[†]

[†]Division of Atmospheric Sciences, Department of Physics, University of Helsinki, P.O. Box 64, 00014 Helsinki, Finland

[‡]Laboratory of Physical Chemistry, Department of Chemistry, University of Helsinki, P.O. Box 55, 00014 Helsinki, Finland

Supporting Information

ABSTRACT: The formation of new particles through condensation from the gas phase is an important source of atmospheric aerosols. The properties of the electrically neutral clusters formed in the very first steps of the condensation process are, however, not directly observable by experimental means. We present here electronic structure calculations on the hydrates of clusters of three molecules of sulfuric acid and three molecules of ammonia or dimethylamine. On the basis of the results of these new calculations together with previously published material we simulate the influence of hydration on the dynamic processes involved in particle formation. Most strongly affected by hydration and most important as a mediator for the effect on particle formation rates are the evaporation rates of clusters. The results give an estimate of the sensitivity of the atmospheric particle formation rate for humidity. The particle formation rate can change approximately two orders of magnitude in either direction due to hydration; the net effect, however, is highly dependent on the exact conditions.

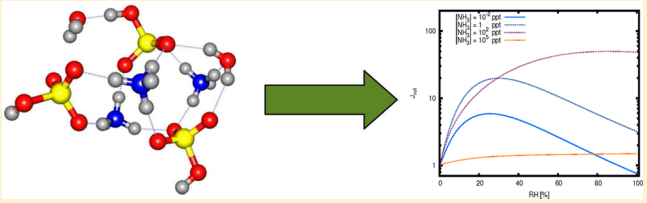

INTRODUCTION

Atmospheric aerosols constitute one of the largest uncertainties in climate and cloud models.[1,2] Also, they can adversely affect health.[3] A large fraction of aerosol particles in the atmosphere is estimated to originate from gas-to-particle transformation.[4]

Sulfuric acid has for a long time been accepted to play a central role in new particle formation under most conditions, and also water is likely to be involved because its concentration exceeds those of other condensable gases often by 8−10 orders of magnitude.[5] Observed formation rates are, however, much higher than would result from binary nucleation of sulfuric acid and water. More recent studies have suggested different species, such as amines,[6,7] ammonia,[8−10] ions,[9,11] or oxidized organic compounds[12,13] to be able to significantly contribute to the particle formation process. In particular, dimethylamine has been shown to at least partially be able to explain atmospheric particle formation rates.[14]

For the description of the very first steps of particle formation that are, at least for electrically neutral clusters, not directly observable by any experimental methods, electronic structure calculations can be utilized. These calculations give detailed information about the structures and relative stabilities of the clusters, which can be used in the direct modeling of the particle formation processes.[15,17] For some systems involving sulfuric acid and amines, a number of studies have been undertaken that also include water molecules, the sulfuric acid/water system[18−25] and both the sulfuric acid/ammonia/water[26−29] and the sulfuric acid/dimethylamine/water systems;[30−33] however, none of these studies presents a sufficiently comprehensive set of clusters to reasonably model particle formation, and the different data sets cannot be combined as they employ different methodologies for electronic structure calculations. We now present new electronic structure calculations on the electrically neutral sulfuric acid/ammonia/water and sulfuric acid/dimethlyamine/water system that complement our previously published set of calculations on these systems.[34] On the basis of these new data we discuss the effects of hydration on both collision and evaporation processes as well as resulting particle formation rates.

THEORETICAL METHODS

Electronic structure calculations on the hydrates of three sulfuric acid/three base clusters (with base being either ammonia or dimethylamine) were performed using the multistep approach elected by Ortega et al.[35] as in our previous article,[34] thus conveniently complementing our existing thermodynamic database.

While an extensive comparison of the reliability of the method used here and several others can be found in ref 36, the error in terms of resulting equilibrium constants can be expected to be approximately one order of magnitude. Trends within the data can, however, be expected to be much more

Received: November 20, 2015
Revised: January 29, 2016
Published: February 26, 2016

DOI: 10.1021/acs.jpca.5b11366
J. Phys. Chem. A 2016, 120, 1886−1896

accurate, as the underlying chemical phenomena are fully covered by the method.

Cluster geometries of the hydrates of clusters containing three sulfuric acid and three base molecules were optimized using a B3LYP functional[37] with CBSB7 (6-311G(2d,d,p)) basis set,[38] as implemented in the Gaussian 09 program package.[39] This way, up to 309 configurations for each cluster, covering different hydrogen-bond donor/acceptor arrangements and protonation states, were sampled. Frequency calculations have been performed on all optimized geometries, confirming them to exhibit no imaginary frequencies. The obtained frequencies were used without scaling for the calculation of Gibbs free energies. On the basis of Gibbs free energy at B3LYP/CBSB7 level, cluster geometries were chosen for single-point calculations covering ∼3 kcal/mol from the lowest energy. Single point energy calculations were performed using the Turbomole program package[40] for the RICC2 method[41] with a aug-cc-pV(T+d)Z[42,43] basis set for sulfur and aug-cc-pVTZ[44−46] for all other atoms.

The Gibbs free energies of hydration obtained from the combination of RICC2 single-point energies with thermal contributions from DFT calculations were converted into equilibrium constants for the formation of the respective hydrate, using only the single lowest energy structure for each cluster composition. The effect of including several configurations via Boltzmann averaging on closely related, negatively charged clusters was recently studied by Tsona et al.[47] and found to be comparatively small in most cases. The obtained equilibrium constants were converted into (relative) equilibrium hydrate populations, using the temperature dependency of the water saturation vapor pressure given by Wexler.[48] This gives the relative population, x_n, of the hydrate containing n water molecules as

$$x_n = \left(\frac{p(\mathrm{H_2O})}{p^0}\right)^n x_0 \mathrm{e}^{-\Delta_{\mathrm{hydr}}G(n)/RT} \tag{1}$$

with the population of the dry cluster x_0 chosen so that $\sum_0^5 x_n = 1$. $p(\mathrm{H_2O})$ is the water partial pressure, p_0 is the reference pressure (1 atm), T is the temperature, and R is the molar gas constant.

For all collisions between, and evaporation/fission processes of all clusters within the simulated system (i.e., containing up to four sulfuric acid molecules, or up to three sulfuric acid molecules together with up to three base (either ammonia or diemthylamine) molecules), collision and evaporation rates were calculated. All studied clusters contain zero to five water molecules, except for the three acid/three base molecule clusters, which contain only up to four water molecules. Of the monomers, only for sulfuric acid was a full set of five hydrates included. For dimethylamine and ammonia only one and four hydrates were included, respectively. Both bases, however, have exclusively positive Gibbs free energies of hydration and thus remain effectively unhydrated. Collision coefficients were calculated from kinetic gas theory, assuming unity sticking factor

$$\beta_{i,j} = \left(\frac{3}{4\pi}\right)^{1/6}\left(\frac{6k_\mathrm{B}T}{m_i} + \frac{6k_\mathrm{B}T}{m_j}\right)^{1/2}(V_i^{1/3} + V_j^{1/3})^2 \tag{2}$$

where k_B is the Boltzmann constant and m_i and V_i are mass and volume of cluster i, respectively. This simple approach essentially neglects three types of possible influences on the collision rates. One of these would be a decrease in effective collision rate due to an energy barrier for cluster formation, which would lead to a sticking factor of less than one. The other influences are deviations in collision rates due to nonsphericity of clusters and due to interactions between particles. To the best of our knowledge, there is no indication of the existence of significant energy barrier for initial particle formation (as opposed to particle reorganization, as is discussed later). While the other two influences would certainly affect the system under study, they are not easily quantifiable. On the basis of studies on the influence of nonsphericity[49] and interactions[50] on collision rates in much simpler systems, it can, however, be estimated that the total enhancement of collision coefficients will be less than one order of magnitude. Using this upper limit of a 10-fold enhancement of the collision coefficient we have tested our system's sensitivity for an enhancement of collision rates. The results (see Supporting Information for details) show no qualitatively different behavior, only a trend toward a slightly stronger lowering effect of hydration on particle formation rates.

Evaporation coefficients were obtained from the corresponding collision rates using equilibrium conditions

$$\gamma_{i,j} = \beta_{i,j}\frac{p^0}{k_\mathrm{B}T}\exp\left(\frac{\Delta G_{i,j} - \Delta G_i - \Delta G_j}{RT}\right) \tag{3}$$

This assumes that the lowest energy structure of each cluster can be formed within the time scale relevant for the simulation, that is, without an energy barrier of at least similar magnitude as the relevant binding energies. While this type of energy barrier for cluster rearrangement processes has been shown to exist for some processes,[51] we believe it is reasonable to assume that for processes involving the rearrangement of hydrates the energy barriers will be of similar magnitude as the corresponding binding energies of water. This would imply that at least for the hydrate structures, which are the subject of this study, rearrangement processes will be fast enough to be neglected in the calculation of evaporation coefficients (cf. the corresponding discussion of collision and evaporation processes involving water molecules later).

The obtained collision and evaporation coefficients were averaged over the hydrate distribution for each cluster composition (in terms of number of acid and base molecules)

$$\beta_{kl,uv} = \sum_{n=0}^{5} x_{kln} \sum_{q=0}^{5} x_{uvq}\beta_{kln,uvq} \tag{4}$$

$$\gamma_{kl,uv} = \sum_{n=0}^{5}\sum_{q=0}^{5-n} x_{(k+u)(l+v)(n+q)}\gamma_{kln,uvq} \tag{5}$$

where k, l, and u, v are the number of sulfuric acid and base molecules and n and q are the number of water molecules, respectively, in the fragment clusters colliding or produced in the evaporation process. The underlying assumption is that processes involving collisions with or evaporations of water molecules are equilibrated within the time scale between collision or evaporation processes involving acid or base molecules, which is based on water molecules being commonly at least eight orders of magnitude more abundant in atmospheric systems than either of the other involved components (which means that collisions, and therefore also close-to-equilibrium evaporations, will happen about eight orders of magnitude more often than for other species).

DOI: 10.1021/acs.jpca.5b11366
J. Phys. Chem. A 2016, 120, 1886−1896

These effective collision and evaporation coefficients were used to solve the birth−death equation for all involved clusters for the steady state. This was done using the Atmospheric Cluster Dynamics Code (ACDC). For details of the ACDC, see refs 15−17. Simulations were performed for the ternary systems (sulfuric acid, water, and ammonia or dimethylamine) for temperatures between T = 263 and 303 K; sulfuric acid concentrations of $[H_2SO_4]$ = 10^5 to 10^9 cm^{-3}, and base concentrations varying from $[NH_3]$ = 10^{-2} to 10^5 ppt and [DMA] = 10^{-5} to 10^2 ppt, respectively. For the binary system (sulfuric acid/water) the temperature range was instead chosen to be T = 193−243 K. The humidity range was in all cases RH = 0 − 100%. While extending this range to supersaturated conditions would be unproblematic for most of the base-containing clusters, for some of the base-free clusters calculation of additional hydrate structures would likely be necessary (cf. ref 34). External sinks were not included in the simulations. The particle formation rate was obtained as the rate of formation of clusters outside the modeled system that (for the base-containing systems) were deemed to have sufficiently stable composition. For the base-free system, this includes all clusters containing at least five sulfuric acid molecules; for the base-containing systems, clusters were required to contain at least four sulfuric acid and a minimum of three base molecules. Although the choice of which clusters to regard as stable is limited by the quantum-chemical data available; judging from previous studies of the dry systems,[17] the choice made here should for the vast majority of the conditions studied include the critical cluster in the dynamic simulations and make certain that the stable cluster is on the main growth pathway of the system. While for the DMA-containing system, commonly no critical cluster exists (i.e., the monomers stand for the maximum in free energy), it cannot be ensured that the critical cluster of the ammonia-containing system lies within the dynamically simulated system for all conditions (combinations of high temperature, low sulfuric acid, and low ammonia concentration might be problematic), especially as the effect of hydration on the identity of the critical cluster has not been systematically studied. Studies of the base-free system were restricted to low temperatures to keep the size of the critical cluster within the modeled range.

RESULTS AND DISCUSSION

The obtained Gibbs free energies of hydration under standard conditions (i.e., the free energies of addition of n water molecules to the corresponding dry cluster) are found in Table 1. For the sulfuric acid−ammonia cluster all of these hydration energies except for the third are negative (a table with the stepwise hydration free energies is found in the Supporting Information); however, the obtained energies are in all cases less negative than the corresponding values for any of the previously studied ammonia containing (or base free) (i.e., $(H_2SO_4)_m(NH_3)_n$ with m = 0−3, n = 0−2, and $n \leq m$, and $(H_2SO_4)_4$) systems. The smaller systems with equal number of sulfuric acid and ammonia molecules were found to be more strongly hydrated than those with one excess molecule of sulfuric acid. This is in contrast with the general trend of hydration becoming more significant with larger numbers of sulfuric acid molecules. Also, this behavior of these smaller clusters was in contrast with that derived from bulk thermodynamics, which in all cases predicted a decrease in hydration with increasing number of ammonia molecules.[34]

Table 1. Calculated Gibbs Free Energies of Hydration at T = 298.15 K and p^0 = 1 atm ($\Delta_{hydr}G^0$) in kcal mol^{-1}

	$n(H_2O)$			
cluster	1	2	3	4
$(H_2SO_4)_3\cdot(NH_3)_3$	−1.47	−3.49	−3.36	−5.84
$(H_2SO_4)_3\cdot(DMA)_3$	0.07	−2.91	−1.57	−3.70

For the dimethylamine-containing systems, two (at standard conditions) endergonic hydration steps are observed. Both of the free energies of addition of the first and third water molecule are positive. While this is likely incidental, it is interesting to note that this pattern of the first and third hydration energy being positive, while the second and fourth are negative, is shared with the cluster containing two sulfuric acid and two DMA molecules. Also, the second and fourth hydration energies of all previously studied smaller DMA-containing clusters are negative. In terms of magnitude, the hydration energies of the dimethylamine containing cluster studied here lie in all cases between the corresponding hydration energies of the previously studied smaller clusters with 1:1 sulfuric acid/dimethylamine composition.

In Figure 1 the structures of the clusters containing three sulfuric acid and three ammonia molecules are depicted. As can be seen, in all cases all ammonia molecules are protonated, whereas all sulfuric acid molecules are singly deprotonated to form bisulfate ions. This is similar to the previously studied clusters with equal numbers of sulfuric acid and ammonia molecules, in which in 11 of 12 clusters one proton is transferred per acid/base pair (the exception being the dry clusters consisting of one of both molecules). A striking structural element is the existence of two sulfuric acid protons that are not participating in hydrogen bonds. This is found in all structures except the trihydrate, which has a notably low stability compared with the other hydrates.

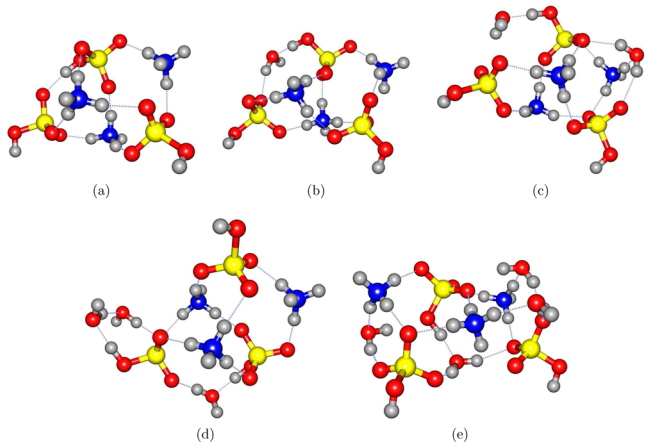

Figure 1. Structures of $(H_2SO_4)_3\cdot(NH_3)_3$ hydrates.

The structures of hydrated clusters containing three sulfuric acid and three dimethylamine molecules are depicted in Figure 2. Also, in these structures all base molecules are protonated, and all sulfuric acid molecules singly deprotonated to form bisulfate ions. In contrast with the ammonia-containing structures, the DMA-containing structures, except for the trihydrate, do not exhibit any sulfuric acid protons that are not involved in hydrogen bonds.

DOI: 10.1021/acs.jpca.5b11366
J. Phys. Chem. A 2016, 120, 1886−1896

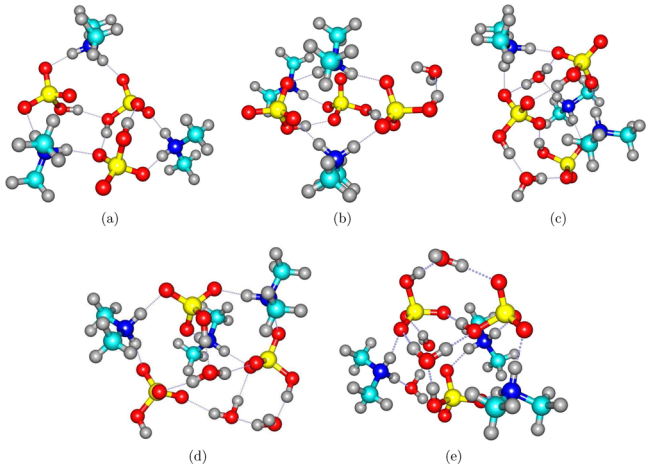

Figure 2. Structures of $(H_2SO_4)_3 \cdot (DMA)_3$ hydrates.

The resulting average hydration of the clusters as a function of relative humidity at room temperature is depicted in Figure 3. Because of the behavior of the hydration energies previously discussed, the average hydration of these clusters is generally lower than that of all clusters previously discussed,[34] except for the two-sulfuric-acid-two-dimethylamine cluster that was essentially unhydrated under all conditions. Also, for clusters containing three ammonia or dimethylamine molecules, no leveling off of the hydration at higher relative humidities is found. This was previously only observed for clusters containing two molecules of dimethylamine.

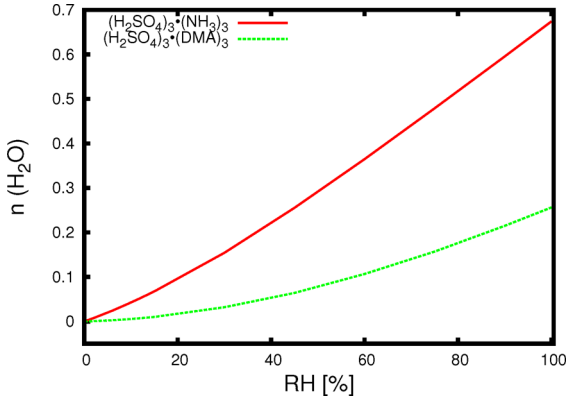

Figure 3. Average hydration numbers for $(H_2SO_4)_3 \cdot (base)_3$ at 298.15 K.

Hydration's Effect on Collision and Evaporation Rates. Because the addition of water molecules to a given cluster increases both its mass and volume, hydration naturally affects the rates of collisions between cluster (see also eq 2). This effect is illustrated in Figure 4 using the rate coefficients for the collisions of the (hydrated) sulfuric acid monomer with all clusters up to a size of two acid and two base molecules. The profile of the rate coefficient for collisions between two sulfuric acid monomers closely resembles the shape of the average hydration of the sulfuric acid monomer. Profiles of the other rate coefficients also have a resemblance of the hydration number profiles of the colliding clusters. In all cases, the shape of the curves is similar to the corresponding hydration number curves (cf. ref 34). This illustrates that, in determining the rate coefficients for hard-sphere collisions, the dominating factor affected by hydration is the size (collision diameter) of the clusters; however, changes in electrostatic interactions due to changes in dipole moments, whose effects are not included in the hard-sphere approximation used here, might lead to deviations from this simple relation. Figures illustrating the dependency of relative collision coefficients on relative humidity for other possible collisions within the system studied are shown in the Supporting Information.

Figure 5a–c illustrates three qualitatively different behaviors of evaporation rates. They show the effect of hydration on the evaporation of the sulfuric acid tetramer, the cluster containing three sulfuric acid and two ammonia molecules, and the cluster containing three sulfuric acid and one dimethylamine molecule, respectively. In each case, all possible evaporation processes are shown individually (though averaged over the hydrate distribution) as well as their sum. It can be seen that under most conditions some specific route is dominating the evaporation process of each cluster; however, three basically different situation can be identified. In the case of the evaporation processes of the sulfuric acid tetramer (Figure 5a), the dominating process changes at very low relative humidity: Under nearly dry conditions (RH < 4%) the fission into two dimers is dominant; at higher relative humidities, the evaporation of a single sulfuric acid molecule is much more important. Similarly, in the case of the cluster containing three sulfuric acid and two ammonia molecules (Figure 5b), the dominant process changes with relative humidity. At low relative humidities the major evaporation process is the loss of a sulfuric acid molecule; at higher humidities (around RH = 30%), evaporation of an ammonia molecule becomes prevalent; however, under none of the simulated conditions does any single process fully dominate the total evaporation rate. The third possible decomposition process, the fission into a cluster containing two acids together with one ammonia molecule and a cluster with one acid and one ammonia molecule, however, is essentially insignificant under all simulated conditions. In the third depicted case, the evaporation of the three-sulfuric-acid-one-dimethylamine-cluster (Figure 5c), the evaporation of a single sulfuric acid molecules is fully dominating the overall process. Both other decomposition processes remain at least six orders of magnitude slower under all conditions, even though they are much more strongly affected by changes in relative humidity.

It should be noted that in contrast with the effect on collision coefficients previously described, the effect on evaporation rates cannot even qualitatively be directly assessed from the average hydration numbers of the cluster involved in the process. While collision coefficients uniformly rise with increasing hydration, evaporation coefficients can both increase and decrease. Furthermore, they do not necessarily do so monotonously, but the direction of change can differ depending on the stability of the hydrates that are predominantly populated at a certain relative humidity. This can be most clearly observed for the processes depicted in Figure 5a but can also be seen for the fission process $((H_2SO_4)_3 \cdot (NH_3)_2 \rightarrow (H_2SO_4)_2 \cdot NH_3 + H_2SO_4 \cdot NH_3)$ in Figure 5b. This implies that while the effect of hydration on collision processes in principle can be realistically modeled using classical methods, the effect on evaporation processes is more complex and requires taking into account stabilities of individual hydrate structures. Also, it should be noted that the effect of hydration on evaporation rates is in nearly all cases much larger than that on collision rates. While changes of the collision coefficients barely span more than 20%,

DOI: 10.1021/acs.jpca.5b11366
J. Phys. Chem. A 2016, 120, 1886–1896

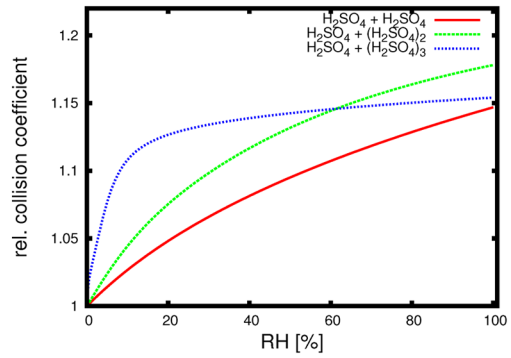

(a) Base-free clusters, dry rate constants $\beta = 3.46 \cdot 10^{-16}$, $3.82 \cdot 10^{-16}$, and $4.21 \cdot 10^{-16}$ cm^3 s^{-1}, respectively.

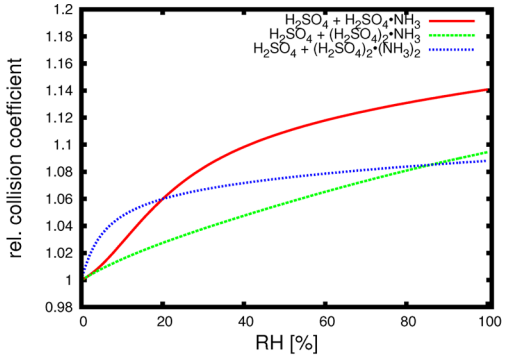

(b) Ammonia-containing clusters, dry rate constants: $\beta = 3.79 \cdot 10^{-16}$, $4.08 \cdot 10^{-16}$, and $4.31 \cdot 10^{-16}$ cm^3 s^{-1}, respectively.

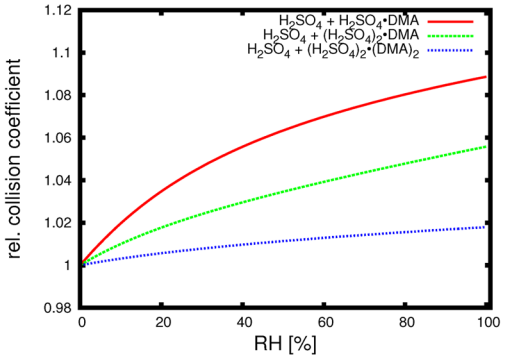

(c) DMA-containing clusters, dry rate constants: $\beta = 4.22 \cdot 10^{-16}$, $4.46 \cdot 10^{-16}$, and $4.97 \cdot 10^{-16}$ cm^3 s^{-1}, respectively.

Figure 4. Relative collision coefficients of (hydrated) sulfuric acid molecules as a function of relative humidity at 298.15 K. Coefficients are relative to the collision coefficients of the corresponding dry clusters.

evaporation coefficients can change by up to three orders of magnitude. Therefore, it can be expected that the effects of hydration on particle formation are predominantly caused by the changes in evaporation rates.

Implications for Particle Formation Rates. For the base-free system the modeled effect of humidity on particle formation is exemplified in Figure 6. As can be seen in the first panel, the presence of water leads in all cases to a higher particle formation rate as compared with the dry case. In the shown case, at 208 K, nearly all of the increase in formation rates happens already at very low relative humidity. In fact, for the lower sulfuric acid concentrations studied ($[H_2SO_4] \leq 10^7$ cm^{-3}) the formation rate reaches a maximum, after which a continuous, though gentle (in the graphical representation barely noticeable), decline is observed. The position of the maximum shifts toward higher relative humidities with increasing sulfuric acid concentration (from 25% RH at $[H_2SO_4] = 10^5$ cm^{-3} to 52% RH at $[H_2SO_4] = 10^7$ cm^{-3}) before disappearing entirely. On the contrary, an increase in acid concentration generally leads to a significantly smaller increase in particle formation rate with humidity. The position and existence of the maximum are also temperature-dependent. The maximum is only observed at temperatures between 198 and 213 K, existing up to higher acid concentrations with rising temperature (at $T = 213$ K up to $[H_2SO_4] = 3 \times 10^7$ cm^{-3}). The maximum is most pronounced in the 208 K case depicted here.

Figure 6b shows the absolute values of the particle formation rate as a function of relative humidity at constant sulfuric acid concentration but different temperatures. The acid concentration is constant at $[H_2SO_4] = 3 \times 10^6$ cm^{-3}. A prominent feature is that the formation rate approaches similar values for all simulated temperatures and levels off at high relative humidities (although at the highest modeled temperatures, formation rates do not level off within the studied humidity range); however, the system does not fully reach the kinetic limit. The existence of maxima in formation rate previously discussed indicates clearly that evaporation processes are still of significance and even have increasing effect at high relative humidities (while collision rates in all cases increase with humidity as previously discussed).

Reflecting the more complex nature of the base-containing systems, with several different possible growth pathways, the humidity dependence of the particle formation rate is more complex for these systems. An overview over the observed qualitative humidity-dependent behaviors of the base-containing systems is given in Table 2. Figure 7 shows the behavior of the base-containing systems for the lowest studied temperature ($T = 263$ K) for both very low ($[H_2SO_4] = 10^5$ cm^{-3}) and high ($[H_2SO_4] = 10^9$ cm^{-3}) sulfuric acid concentration. Figure 7a especially illustrates well the multitude of observed changes in the formation rate. Under the conditions depicted here ($T = 263$ K and $[H_2SO_4] = 10^5$ cm^{-3}) at comparatively low ammonia concentrations ($NH_3 < 10^3$ ppt) the particle formation rate initially increases with relative humidity, to

DOI: 10.1021/acs.jpca.5b11366
J. Phys. Chem. A 2016, 120, 1886−1896

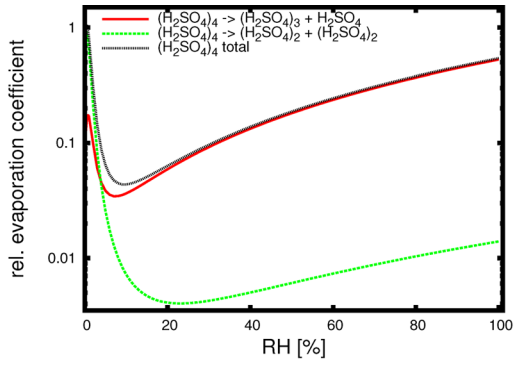

(a) $(H_2SO_4)_4$, dry total rate constant $\gamma = 7.52 \cdot 10^4$ s^{-1}

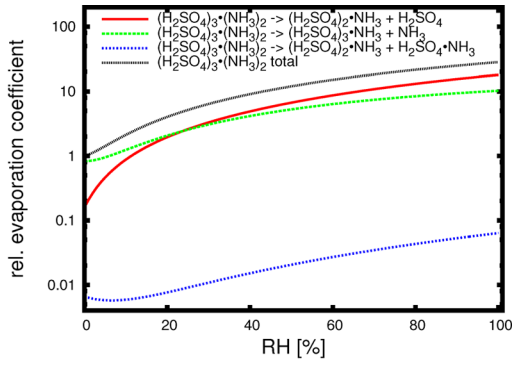

(b) $(H_2SO_4)_3 \cdot (NH_3)_2$, dry total rate constant $\gamma = 1.07 \cdot 10^{-1}$ s^{-1}

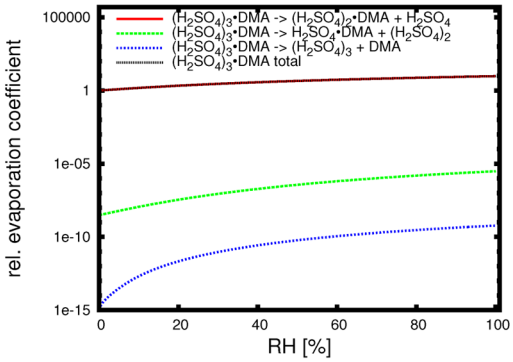

(c) $(H_2SO_4)_3 \cdot$ DMA, dry total rate constant $\gamma = 3.67$ s^{-1}

Figure 5. Relative evaporation coefficients of clusters as a function of relative humidity. Coefficients for individual processes are relative to the sum of all individual coefficients for the dry cluster. Here shown for 298.15 K. The humidity dependence is qualitatively similar at all studied temperatures; absolute values are, however, strongly temperature-dependent.

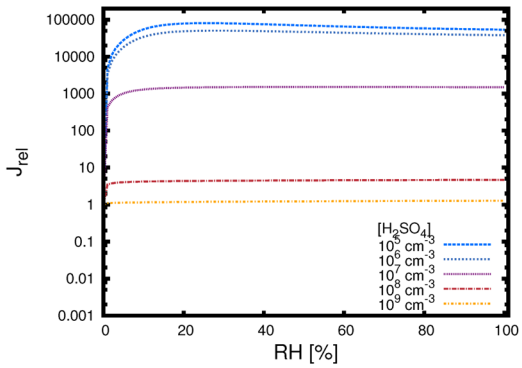

(a) relative rate, $T = 208$ K, dry rates $J = 3.68 \cdot 10^{-10}$, $3.69 \cdot 10^{-5}$, 3.78, $2.09 \cdot 10^5$, and $7.69 \cdot 10^7$ cm^{-3} s^{-1}, respectively.

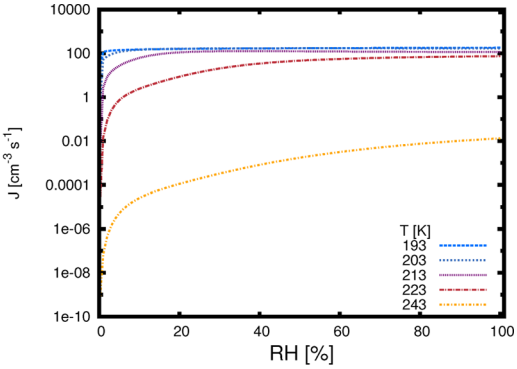

(b) absolute rate, $[H_2SO_4] = 3 \cdot 10^6$ cm^{-3}

Figure 6. Modeled (relative) particle formation rate in the base-free system as a function of relative humidity.

reach a maximum that can be nearly two orders of magnitude above the dry particle formation rate. The existence of this maximum can be attributed to the rise in evaporation coefficients of the $(H_2SO_4)_2 \cdot NH_3$, $(H_2SO_4)_3 \cdot (NH_3)_2$, and $(H_2SO_4)_3 \cdot (NH_3)_3$ clusters, which all display similar absolute values and changes with humidity. As previously described, changes in evaporation rates due to hydration are commonly much larger than in collision rates, so that the increasing evaporation rates can become determining above a threshold, which depends on the conditions. The relative humidity at which this maximum is reached increases with increasing ammonia concentration, the height of the maximum, however, peaks at NH_3 = 10 ppt. For the lowest simulated ammonia concentrations, the formation rates subsequently decrease, even below the value under dry conditions. While at low ammonia concentrations ($NH_3 \leq 10$ ppt) the initial slope of the formation rate increases with ammonia concentration, it decreases at higher concentrations to give a very flat curve, indicating a small but continuous increase in particle formation rate with relative humidity for the highest ammonia concentrations.

DOI: 10.1021/acs.jpca.5b11366
J. Phys. Chem. A 2016, 120, 1886−1896

Table 2. Qualitative Overview over Humidity Dependency of the Particle Formation Rates in the Base Containing Systems[a]

		[NH_3]			[DMA]		
temperature	[H_2SO_4]	low	intermediate	high	low	intermediate	high
low	low	+−	+−	+	+	+	+
	high	+−	+	+	+	+	+
intermediate	intermediate	−	+−	+	+−	+	+
high	low	−	−	+−	+−	+−	−
	high	−	+−	+	−	+−	+

[a]+, monotonous increase; −, monotonous decrease; +−, increase that is followed by a maximum and decrease. It should be noted that the changes in the dimethylamine-containing system are generally much smaller than in the ammonia-containing system.

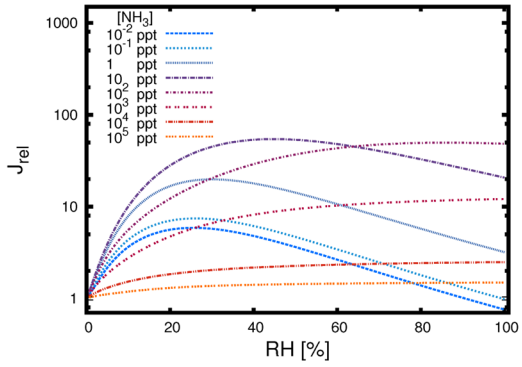

(a) $[H_2SO_4] = 10^5$ cm^{-3}, base = NH_3, dry rates $J = 3.95 \cdot 10^{-15}$, $3.03 \cdot 10^{-12}$, $9.10 \cdot 10^{-10}$, $1.08 \cdot 10^{-7}$, $7.26 \cdot 10^{-6}$, $1.54 \cdot 10^{-4}$, $9.81 \cdot 10^{-4}$, and $1.78 \cdot 10^{-3}$ cm^{-3} s^{-1}, respectively.

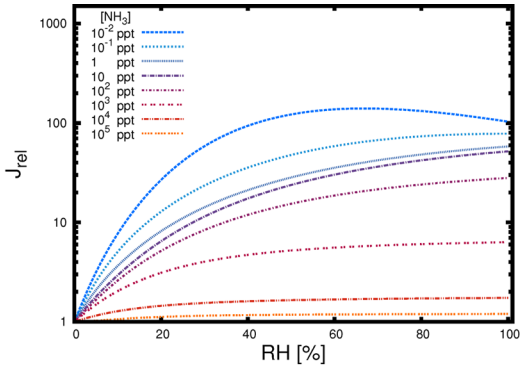

(b) $[H_2SO_4] = 10^9$ cm^{-3}, base = NH_3, dry rates $J = 1.03$, $2.85 \cdot 10^2$, $1.24 \cdot 10^4$, $2.11 \cdot 10^5$, $2.34 \cdot 10^6$, $2.01 \cdot 10^7$, $8.51 \cdot 10^7$, and $1.30 \cdot 10^8$ cm^{-3} s^{-1}, respectively.

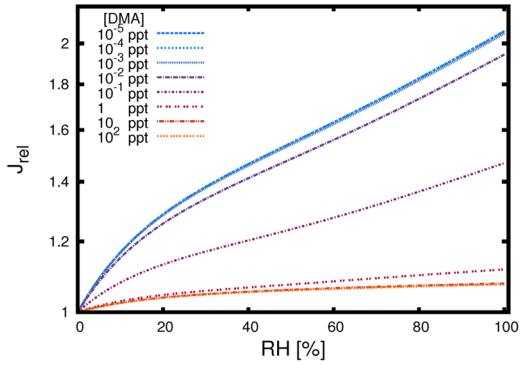

(c) $[H_2SO_4] = 10^5$ cm^{-3}, base = DMA, dry rates $J = 8.03 \cdot 10^{-15}$, $8.01 \cdot 10^{-12}$, $7.78 \cdot 10^{-9}$, $5.90 \cdot 10^{-6}$, $8.51 \cdot 10^{-4}$, $3.61 \cdot 10^{-3}$, $4.01 \cdot 10^{-3}$, and $4.04 \cdot 10^{-3}$ cm^{-3} s^{-1}, respectively.

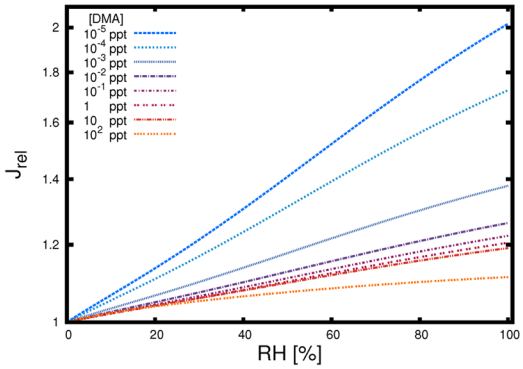

(d) $[H_2SO_4] = 10^9$ cm^{-3}, base = DMA, dry rates $J = 4.73 \cdot 10^{-2}$, 22.6, $1.62 \cdot 10^3$, $3.07 \cdot 10^4$, $3.88 \cdot 10^5$, $4.52 \cdot 10^6$, $4.30 \cdot 10^7$, and $1.37 \cdot 10^8$ cm^{-3} s^{-1}, respectively.

Figure 7. Modeled relative particle formation rate as a function of relative humidity at 263 K.

At higher sulfuric acid concentration ($[H_2SO_4] = 10^9$ cm^{-3}, Figure 7b) the behavior of the ammonia-containing system is generally shifted toward the behavior previously observed for high ammonia concentration. Only at the lowest modeled ammonia concentration is a maximum observed at fairly high relative humidities. At all higher ammonia concentrations the curve becomes less steep but monotonously rising. Interestingly, at high acid concentration combined with low ammonia concentrations the maximum increase in the particle formation rate due to hydration is significantly higher than in the low sulfuric acid concentration case. At high ammonia concentrations, however, the increase due to hydration is smaller at high than at low sulfuric acid concentrations.

The system containing dimethylamine at T = 263 K (Figure 7c,d) generally resembles the high base concentration case of the ammonia-containing system. Over the whole humidity range the formation rates increase monotonously, with higher base concentration, leading to a smaller increase, and the largest observed increase being of a factor ∼2. In principle this can be rationalized by dimethylamine both being a much stronger base and affecting the hygroscopicity of clusters much more strongly than ammonia, therefore giving already at low dimethylamine concentrations an effect that is observed at very high ammonia concentrations; however, at the lower sulfuric acid concentration (Figure 7c) nearly all variation of the humidity dependence takes place over an intermediate range of dimethylamine concentrations. Both up to

DOI: 10.1021/acs.jpca.5b11366
J. Phys. Chem. A 2016, 120, 1886−1896

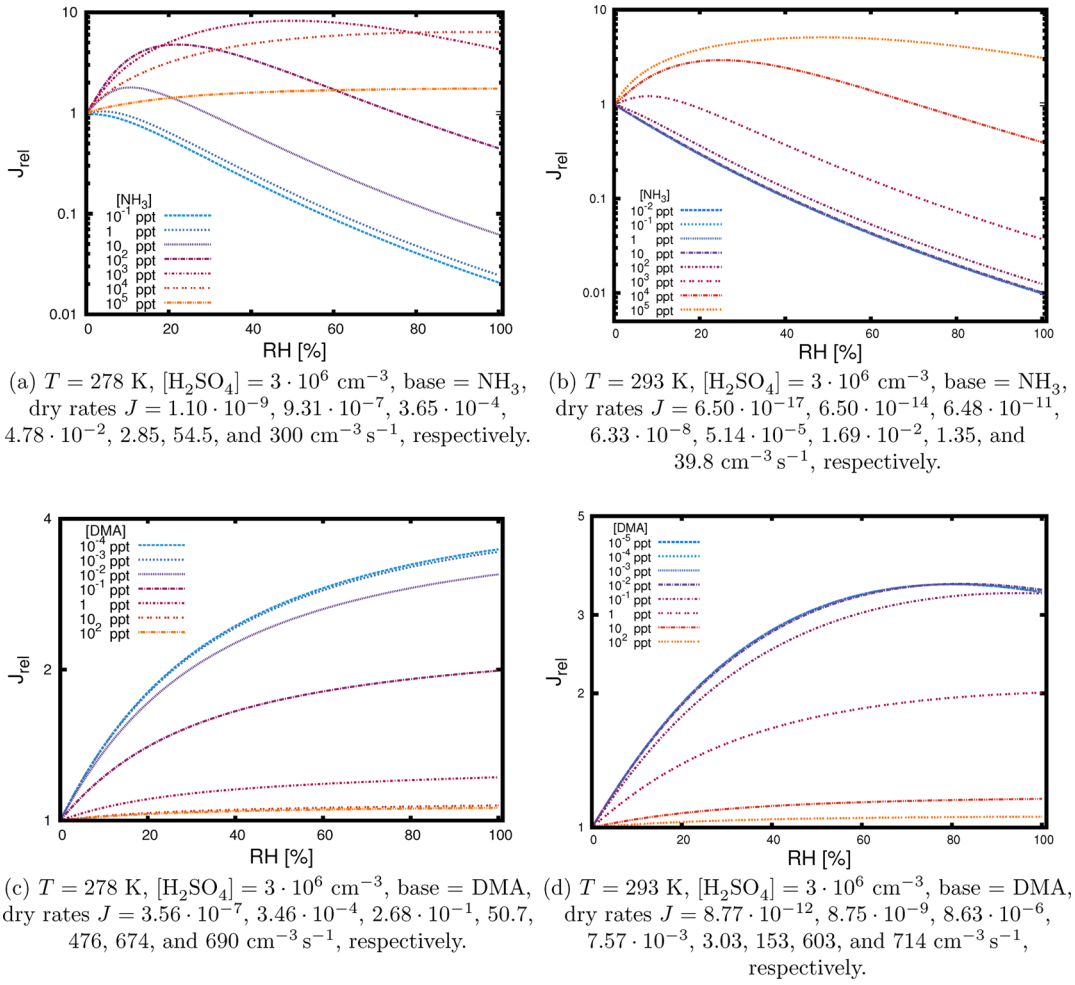

(a) $T = 278$ K, $[H_2SO_4] = 3 \cdot 10^6$ cm^{-3}, base = NH_3, dry rates $J = 1.10 \cdot 10^{-9}$, $9.31 \cdot 10^{-7}$, $3.65 \cdot 10^{-4}$, $4.78 \cdot 10^{-2}$, 2.85, 54.5, and 300 cm^{-3} s^{-1}, respectively.

(b) $T = 293$ K, $[H_2SO_4] = 3 \cdot 10^6$ cm^{-3}, base = NH_3, dry rates $J = 6.50 \cdot 10^{-17}$, $6.50 \cdot 10^{-14}$, $6.48 \cdot 10^{-11}$, $6.33 \cdot 10^{-8}$, $5.14 \cdot 10^{-5}$, $1.69 \cdot 10^{-2}$, 1.35, and 39.8 cm^{-3} s^{-1}, respectively.

(c) $T = 278$ K, $[H_2SO_4] = 3 \cdot 10^6$ cm^{-3}, base = DMA, dry rates $J = 3.56 \cdot 10^{-7}$, $3.46 \cdot 10^{-4}$, $2.68 \cdot 10^{-1}$, 50.7, 476, 674, and 690 cm^{-3} s^{-1}, respectively.

(d) $T = 293$ K, $[H_2SO_4] = 3 \cdot 10^6$ cm^{-3}, base = DMA, dry rates $J = 8.77 \cdot 10^{-12}$, $8.75 \cdot 10^{-9}$, $8.63 \cdot 10^{-6}$, $7.57 \cdot 10^{-3}$, 3.03, 153, 603, and 714 cm^{-3} s^{-1}, respectively.

Figure 8. Modeled relative particle formation rate as a function of relative humidity at intermediate temperatures and sulfuric acid concentrations.

[DMA] = 10^{-3} ppt and again from [DMA] = 10 ppt the curves change only minimally with varying dimethylamine concentration; the largest part of the total variation takes place from [DMA] = 10^{-2} to 1 ppt. At the higher sulfuric acid concentration, the change happens over the whole span of dimethylamine concentrations and is actually largest in the extreme ends of the concentration range.

Figure 8 shows the humidity dependence of the relative particle formation rate in both base-containing systems at an intermediate sulfuric acid concentration and two different elevated temperatures to illustrate the variation of the humidity dependence with temperature. For the ammonia-containing system it becomes clear that at these higher temperatures the maximum in particle formation rates is shifted toward lower relative humidities, even so far that at low ammonia concentration it disappears entirely, and the formation rate decreases over the whole humidity range. At T = 278 K (Figure 8a) no maximum is observed at concentrations below [NH_3] = 1 ppt, and at T = 293 K even [NH_3] = 10^3 ppt is required to give a maximum. Similarly, the upper limit of the ammonia concentration, at which a maximum is still observed within the studied humidity range, is shifted toward higher RH values. At T = 278 K the maximum disappears only at the highest simulated ammonia concentration (at [NH_3] = 10^4 ppt a maximum is still reached at RH = 95%); at T = 293 K, even the highest ammonia concentration gives a maximum for the formation rate. Also, in agreement with the decreasing trend in the formation rate with increasing humidity, the maximum increase that is observed becomes smaller at these temperatures and is below 1 order of magnitude. Furthermore, at high temperatures, significant changes in the humidity dependence of the formation rate with increasing ammonia concentration are only observed above a certain threshold. At T = 278 K, a change is first noticed at [NH_3] = 1 ppt; at T = 293 K, a change is first noticed at [NH_3] = 10^2 ppt.

The behavior of the dimethylamine-containing system at these elevated temperatures becomes more similar to that of the low-temperature ammonia-containing system; the maximum increase in formation rate is larger than that at T = 263 K. Also, for the lowest dimethylamine concentrations at T = 293 K a maximum in the humidity-dependent change of the particle formation rate is observed. A similarity with the ammonia-containing system at the same temperatures, however, is that close to the lowest modeled base concentrations the curves are barely affected by a chang in the base concentration.

At the highest modeled temperature at low acid concentration (T = 303 K, [H_2SO_4] = 10^5 cm^{-3}, Figure 9a), for the ammonia-containing system, the trend previously ascribed to the temperature rise, continues. Only at the lowest ammonia concentration ([NH_3] = 10^{-2} ppt) is a maximum in the humidity-dependent particle formation rate observed. At all higher ammonia concentrations the formation rate decreases monotonically. Also, the relative formation rates are generally

DOI: 10.1021/acs.jpca.5b11366
J. Phys. Chem. A 2016, 120, 1886−1896

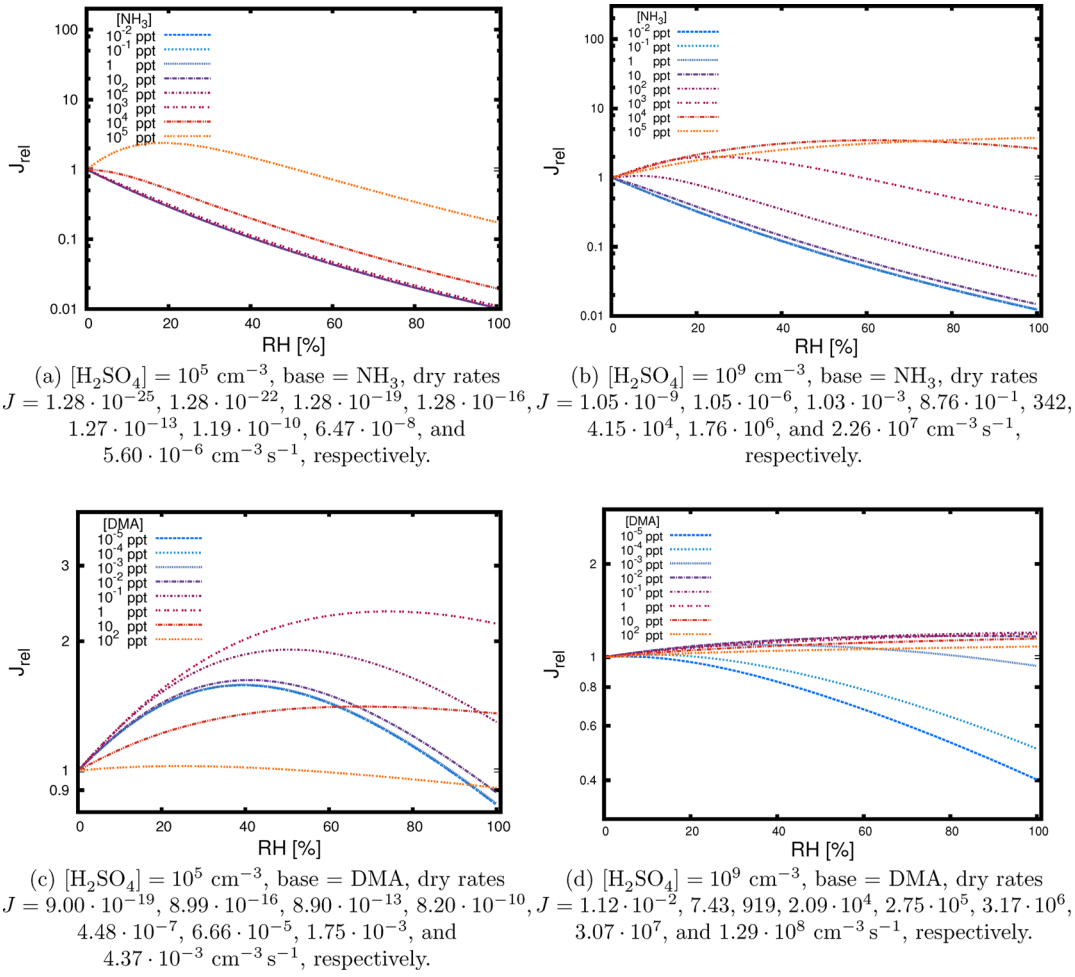

(a) $[H_2SO_4] = 10^5$ cm^{-3}, base = NH_3, dry rates $J = 1.28 \cdot 10^{-25}$, $1.28 \cdot 10^{-22}$, $1.28 \cdot 10^{-19}$, $1.28 \cdot 10^{-16}$, $1.27 \cdot 10^{-13}$, $1.19 \cdot 10^{-10}$, $6.47 \cdot 10^{-8}$, and $5.60 \cdot 10^{-6}$ cm^{-3} s^{-1}, respectively.

(b) $[H_2SO_4] = 10^9$ cm^{-3}, base = NH_3, dry rates $J = 1.05 \cdot 10^{-9}$, $1.05 \cdot 10^{-6}$, $1.03 \cdot 10^{-3}$, $8.76 \cdot 10^{-1}$, 342, $4.15 \cdot 10^4$, $1.76 \cdot 10^6$, and $2.26 \cdot 10^7$ cm^{-3} s^{-1}, respectively.

(c) $[H_2SO_4] = 10^5$ cm^{-3}, base = DMA, dry rates $J = 9.00 \cdot 10^{-19}$, $8.99 \cdot 10^{-16}$, $8.90 \cdot 10^{-13}$, $8.20 \cdot 10^{-10}$, $4.48 \cdot 10^{-7}$, $6.66 \cdot 10^{-5}$, $1.75 \cdot 10^{-3}$, and $4.37 \cdot 10^{-3}$ cm^{-3} s^{-1}, respectively.

(d) $[H_2SO_4] = 10^9$ cm^{-3}, base = DMA, dry rates $J = 1.12 \cdot 10^{-2}$, 7.43, 919, $2.09 \cdot 10^4$, $2.75 \cdot 10^5$, $3.17 \cdot 10^6$, $3.07 \cdot 10^7$, and $1.29 \cdot 10^8$ cm^{-3} s^{-1}, respectively.

Figure 9. Modeled relative particle formation rate as a function of relative humidity at 303 K.

lower than at lower temperatures, leading to a maximum increase of less than a factor of three and a maximum decline of nearly two orders of magnitude. Furthermore, the ammonia concentration required to achieve a significant change in the humidity-dependent behavior of the system, below $[NH_3] = 10^4$ ppt, characteristics of the curves changes only marginally. At high sulfuric acid concentration on the contrary (Figure 9b), the variation with ammonia concentration is increased. While at the highest ammonia concentration the behavior is similar to that at much lower temperatures, giving a steady minor increase in the particle formation rate with humidity, it resembles at low ammonia concentration that of the low sulfuric acid system at the same temperature. Also, here it can be noted that a certain threshold ammonia concentration of $[NH_3] = 10$ ppt needs to be overcome to observe a significant effect. From $[NH_3] = 10^2$ ppt to $[NH_3] = 10^4$ ppt a maximum in the relative humidity is observed within the humidity range studied.

Also, for this highest temperature modeled, the dimethylamine-containing system behaves similar to the ammonia-containing system at a lower temperature. At the lowest sulfuric acid concentration the formation rate initially increases at all base concentrations to go through a maximum, as shown in Figure 9c. The relative humidity at which this maximum is reached increases with dimethylamine concentration up to [DMA] = 1 ppt. At concentrations higher than this the curves become generally more flat, and the maximum shifts toward lower relative humidity values. This combination of effects results in the particle formation rate decreasing at high relative humidities compared with the dry case at both ends of the dimethylamine concentration range studied. The largest changes are observed at intermediate base concentrations. At high sulfuric acid concentration (Figure 9d), barely any increase with relative humidity is observed for the dimethylamine-containing system. Although the formation rates (very gently) increase at all modeled base concentrations initially with increasing humidity, the largest increase is ~20% at [DMA] = 10^{-1} ppt. At higher dimethylamine concentrations even under these conditions the curves become more flat, and at lower concentrations the formation rates reach a maximum, after which they decrease often more sharply than the initial increase. Consequently, the largest total change in the formation rate (a factor of ~2.5 close to 100% RH) is observed for the lowest dimethylamine concentration.

CONCLUSIONS

We have presented a set of new calculations on the stability of clusters containing three sulfuric acid, three base molecules (either ammonia or dimethylamine), and up to four water molecules. These new data complement our previous studies on hydrated sulfuric acid/ammonia and sulfuric acid/diemthylamine clusters. With the completed set of data we were able to model the effect of hydration of the clusters on the processes involved in the first steps of particle formation.

DOI: 10.1021/acs.jpca.5b11366
J. Phys. Chem. A 2016, 120, 1886−1896

Collision rates are invariably enhanced by hydration of the clusters, corresponding to the increase in size due to the water uptake of the clusters. Therefore, the effect is strongest for base-free clusters and smallest for DMA-containing clusters. In total, the effect of hydration on collision rates is, however, small, ranging up to ∼20%. The effect of hydration on evaporation rates, on the contrary, is not possible to predict straightforwardly from the average hydration numbers of the clusters. Also, it is in many cases much larger than the effect on collision rates, sometimes ranging several orders of magnitude in either direction. Moreover, in some cases hydration of a cluster can lead to the main route of evaporation changing.

The importance of the change in evaporation rates becomes evident in the simulations of particle formation in the sulfuric acid/ammonia system. Strongly dependent on the exact set of conditions the particle formation rate can change approximately two orders of magnitude in either direction compared with the dry case. For the sulfuric acid/dimethylamine system the resulting changes are generally much smaller and follow in most cases the small increase with rising humidity determined by the change in collision rates. Only at elevated temperatures can evaporations in this system become sufficiently relevant to dominate the overall process, leading to declining particle formation rates only under a few specific sets of conditions. Also, for this system, the total change compared with the dry case is limited to approximately one order of magnitude.

The hydration-dependent behavior of the systems containing the two different bases is similar in the sense that situations with very high ammonia concentrations resemble systems containing dimethylamine. On the basis of this, the two bases can be assumed to be representative of other substances with varying hydrophobicity, able to stabilize sulfuric acid clusters to different degrees, thus providing a more general estimate of the sensitivity of atmospheric particle formation rates to changes in relative humidity.

■ ASSOCIATED CONTENT

Supporting Information

The Supporting Information is available free of charge on the ACS Publications website at DOI: 10.1021/acs.jpca.5b11366.

Cartesian coordinates of all optimized structures; cluster formation Gibbs free energies, enthalpies, and entropies; stepwise hydration free energies; and hydration profiles. Evaporation and collision coefficients as a function of relative humidity for all modeled clusters. Particle formation rate curves for all modeled conditions. (PDF)

■ AUTHOR INFORMATION

Corresponding Author

*E-mail: henning.henschel@helsinki.fi.

Notes

The authors declare no competing financial interest.

■ ACKNOWLEDGMENTS

We thank Oona Kupiainen-Määttä and Tinja Olenius for help with the ACDC software and valuable comments on the mansucript. We gratefully acknowledge ERC StG 257360 MOCAPAF, the Academy of Finland (Center of Excellence program project #272041, and LASTU program project #135054, and project #266388) for funding. We thank the CSC−IT Center for Science in Espoo, Finland, for computing time.

■ REFERENCES

(1) Lohmann, U.; Feichter, J. Global indirect aerosol effects: a review. *Atmos. Chem. Phys.* **2005**, *5*, 715−737.

(2) Kazil, J.; Stier, P.; Zhang, K.; Quaas, J.; Kinne, S.; O'Donnell, D.; Rast, S.; Esch, M.; Ferrachat, S.; Lohmann, U.; et al. Aerosol nucleation and its role for clouds and Earth's radiative forcing in the aerosol-climate model ECHAM5-HAM. *Atmos. Chem. Phys.* **2010**, *10*, 10733−10752.

(3) Lelieveld, J.; Evans, J. S.; Fnais, M.; Giannadaki, D.; Pozzer, A. The contribution of outdoor air pollution sources to premature mortality on a global scale. *Nature* **2015**, *525*, 367−371.

(4) Merikanto, J.; Spracklen, D. V.; Mann, G. W.; Pickering, S. J.; Carslaw, K. S. Impact of nucleation on global CCN. *Atmos. Chem. Phys.* **2009**, *9*, 8601−8616.

(5) Weber, R. J.; Marti, J. J.; McMurry, P. H.; Eisele, F. L.; Tanner, D. J.; Jefferson, A. Measured atmospheric new particle formation rates: implications for nucleation mechanisms. *Chem. Eng. Commun.* **1996**, *151*, 53−64.

(6) Murphy, S. M.; Sorooshian, A.; Kroll, J. H.; Ng, N. L.; Chhabra, P.; Tong, C.; Surratt, J. D.; Knipping, E.; Flagan, R. C.; Seinfeld, J. H. Secondary aerosol formation from atmospheric reactions of aliphatic amines. *Atmos. Chem. Phys.* **2007**, *7*, 2313−2337.

(7) Kurtén, T.; Loukonen, V.; Vehkamäki, H.; Kulmala, M. Amines are likely to enhance neutral and ion-induced sulfuric acid-water nucleation in the atmosphere more effectively than ammonia. *Atmos. Chem. Phys.* **2008**, *8*, 4095−4103.

(8) Ziereis, H.; Arnold, F. Gaseous ammonia and ammonium ions in the free troposphere. *Nature* **1986**, *321*, 503−505.

(9) Kirkby, J.; Curtius, J.; Almeida, J.; Dunne, E.; Duplissy, J.; Ehrhart, S.; Franchin, A.; Gagne, S.; Ickes, L.; Kurten, A.; et al. Role of sulphuric acid, ammonia and galactic cosmic rays in atmospheric aerosol nucleation. *Nature* **2011**, *476*, 429−433.

(10) Schobesberger, S.; Franchin, A.; Bianchi, F.; Rondo, L.; Duplissy, J.; Kürten, A.; Ortega, I. K.; Metzger, A.; Schnitzhofer, R.; Almeida, J.; et al. On the composition of ammonia-sulfuric-acid ion clusters during aerosol particle formation. *Atmos. Chem. Phys.* **2015**, *15*, 55−78.

(11) Yu, F. From molecular clusters to nanoparticles: second-generation ion-mediated nucleation model. *Atmos. Chem. Phys.* **2006**, *6*, 5193−5211.

(12) Metzger, A.; Verheggen, B.; Dommen, J.; Duplissy, J.; Prevot, A. S. H.; Weingartner, E.; Riipinen, I.; Kulmala, M.; Spracklen, D. V.; Carslaw, K. S.; et al. Evidence for the role of organics in aerosol particle formation under atmospheric conditions. *Proc. Natl. Acad. Sci. U. S. A.* **2010**, *107*, 6646−6651.

(13) Schobesberger, S.; Junninen, H.; Bianchi, F.; Lönn, G.; Ehn, M.; Lehtipalo, K.; Dommen, J.; Ehrhart, S.; Ortega, I. K.; Franchin, A.; et al. Molecular understanding of atmospheric particle formation from sulfuric acid and large oxidized organic molecules. *Proc. Natl. Acad. Sci. U. S. A.* **2013**, *110*, 17223−17228.

(14) Almeida, J.; Schobesberger, S.; Kürten, A.; Ortega, I. K.; Kupiainen-Määttä, O.; Praplan, A. P.; Adamov, A.; Amorim, A.; Bianchi, F.; Breitenlechner, M.; David, A.; et al. *Nature* **2013**, *502*, 359−363.

(15) McGrath, M. J.; Olenius, T.; Ortega, I. K.; Loukonen, V.; Paasonen, P.; Kurtén, T.; Kulmala, M.; Vehkamäki, H. Atmospheric Cluster Dynamics Code: a flexible method for solution of the birth-death equations. *Atmos. Chem. Phys.* **2012**, *12*, 2345−2355.

(16) Paasonen, P.; Olenius, T.; Kupiainen, O.; Kurtén, T.; Petäjä, T.; Birmili, W.; Hamed, A.; Hu, M.; Huey, L. G.; Plass-Duelmer, C.; et al. On the formation of sulphuric acid - amine clusters in varying atmospheric conditions and its influence on atmospheric new particle formation. *Atmos. Chem. Phys.* **2012**, *12*, 9113−9133.

(17) Olenius, T.; Kupiainen-Määttä, O.; Ortega, I. K.; Kurten, T.; Vehkamäki, H. Free energy barrier in the growth of sulfuric acid-

ammonia and sulfuric acid-dimethylamine clusters. *J. Chem. Phys.* **2013**, *139*, 084312.
(18) Bandy, A. R.; Ianni, J. C. Study of the hydrates of H2SO4 using density functional theory. *J. Phys. Chem. A* **1998**, *102*, 6533−6539.
(19) Re, S.; Osamura, Y.; Morokuma, K. Coexistence of neutral and ion-pair clusters of hydrated sulfuric acid H2SO4(H2O)n (n = 1−5) A molecular orbital study. *J. Phys. Chem. A* **1999**, *103*, 3535−3547.
(20) Ianni, J.; Bandy, A. A theoretical study of the hydrates of $(H_2SO_4)_2$ and its implications for the formation of new atmospheric particles. *J. Mol. Struct.: THEOCHEM* **2000**, *497*, 19−37.
(21) Ding, C.-G.; Laasonen, K.; Laaksonen, A. Two sulfuric acids in small water clusters. *J. Phys. Chem. A* **2003**, *107*, 8648−8658.
(22) (a) Al Natsheh, A.; Nadykto, A. B.; Mikkelsen, K. V.; Yu, F.; Ruuskanen, J. Sulfuric acid and sulfuric acid hydrates in the gas phase: A DFT investigation. *J. Phys. Chem. A* **2004**, *108*, 8914−8929. (b) Al Natsheh, A.; Nadykto, A. B.; Mikkelsen, K. V.; Yu, F.; Ruuskanen, J. Sulfuric acid and sulfuric acid hydrates in the gas phase: A DFT investigation. *J. Phys. Chem. A* **2006**, *110*, 7982−7984.
(23) Kurtén, T.; Noppel, M.; Vehkamäki, H.; Salonen, M.; Kulmala, M. Quantum chemical studies of hydrate formation of H_2SO_4 and HSO_4^-. *Boreal Environ. Res.* **2007**, *12*, 431−453.
(24) Temelso, B.; Morrell, T. E.; Shields, R. M.; Allodi, M. A.; Wood, E. K.; Kirschner, K. N.; Castonguay, T. C.; Archer, K. A.; Shields, G. C. Quantum mechanical study of sulfuric acid hydration: Atmospheric implications. *J. Phys. Chem. A* **2012**, *116*, 2209−2224.
(25) Temelso, B.; Phan, T. N.; Shields, G. C. Computational study of the hydration of sulfuric acid dimers: Implications for acid dissociation and aerosol formation. *J. Phys. Chem. A* **2012**, *116*, 9745−9758.
(26) Ianni, J. C.; Bandy, A. R. A Density functional theory study of the hydrates of $NH_3{\cdot}H_2SO_4$ and its implications for the formation of new atmospheric particles. *J. Phys. Chem. A* **1999**, *103*, 2801−2811.
(27) Larson, L. J.; Largent, A.; Tao, F.-M. Structure of the sulfuric acid-ammonia system and the effect of water molecules in the gas phase. *J. Phys. Chem. A* **1999**, *103*, 6786−6792.
(28) Nadykto, A. B.; Yu, F. Strong hydrogen bonding between atmospheric nucleation precursors and common organics. *Chem. Phys. Lett.* **2007**, *435*, 14−18.
(29) Kurtén, T.; Torpo, L.; Ding, C.-G.; Vehkamäki, H.; Sundberg, M. R.; Laasonen, K.; Kulmala, M. A density functional study on water-sulfuric acid-ammonia clusters and implications for atmospheric cluster formation. *J. Geophys. Res.* **2007**, *112*, D04210−D04210.
(30) Loukonen, V.; Kurtén, T.; Ortega, I. K.; Vehkamäki, H.; Pádua, A. A. H.; Sellegri, K.; Kulmala, M. Enhancing effect of dimethylamine in sulfuric acid nucleation in the presence of water - a computational study. *Atmos. Chem. Phys.* **2010**, *10*, 4961−4974.
(31) Nadykto, A. B.; Yu, F.; Jakovleva, M. V.; Herb, J.; Xu, Y. Amines in the Earth's atmosphere: A density functional theory study of the thermochemistry of pre-nucleation clusters. *Entropy* **2011**, *13*, 554−569.
(32) Nadykto, A. B.; Herb, J.; Yu, F.; Xu, Y. Enhancement in the production of nucleating clusters due to dimethylamine and large uncertainties in the thermochemistry of amine-enhanced nucleation. *Chem. Phys. Lett.* **2014**, *609*, 42−49.
(33) Kupiainen-Määttä, O.; Henschel, H.; Kurtén, T.; Loukonen, V.; Olenius, T.; Paasonen, P.; Vehkamäki, H. Comment on Enhancement in the production of nucleating clusters due to dimethylamine and large uncertainties in the thermochemistry of amineenhanced nucleation' by Nadykto et al, Chem. Phys. Lett. 609 (2014) 42−49. *Chem. Phys. Lett.* **2015**, *624*, 107−110.
(34) Henschel, H.; Navarro, J. C. A.; Yli-Juuti, T.; Kupiainen-Määttä, O.; Olenius, T.; Ortega, I. K.; Clegg, S. L.; Kurtén, T.; Riipinen, I.; Vehkamäki, H. Hydration of atmospherically relevant molecular clusters: Computational chemistry and classical thermodynamics. *J. Phys. Chem. A* **2014**, *118*, 2599−2611.
(35) Ortega, I. K.; Kupiainen, O.; Kurtén, T.; Olenius, T.; Wilkman, O.; McGrath, M. J.; Loukonen, V.; Vehkamäki, H. From quantum chemical formation free energies to evaporation rates. *Atmos. Chem. Phys.* **2012**, *12*, 225−235.
(36) Leverentz, H. R.; Siepmann, J. I.; Truhlar, D. G.; Loukonen, V.; Vehkamäki, H. Energetics of atmospherically implicated clusters made of sulfuric acid, ammonia, and dimethyl amine. *J. Phys. Chem. A* **2013**, *117*, 3819−3825.
(37) Becke, A. D. Density-functional thermochemistry. III. The role of exact exchange. *J. Chem. Phys.* **1993**, *98*, 5648−5652.
(38) Montgomery, J. A.; Frisch, M. J.; Ochterski, J. W.; Petersson, G. A. A complete basis set model chemistry. VI. Use of density functional geometries and frequencies. *J. Chem. Phys.* **1999**, *110*, 2822−2827.
(39) Frisch, M. J.; Trucks, G. W.; Schlegel, H. B.; Scuseria, G. E.; Robb, M. A.; Cheeseman, J. R.; Scalmani, G.; Barone, V.; Mennucci, B.; Petersson, G. A.; et al. *Gaussian 09*, revision C.1.; Gaussian, Inc.: Wallingford, CT, 2009.
(40) TURBOMOLE V6.3 2011, a development of University of Karlsruhe and Forschungszentrum Karlsruhe GmbH, 1989−2007, TURBOMOLE GmbH, since 2007; available from http://www.turbomole.com.
(41) Christiansen, O.; Koch, H.; Jørgensen, P. The second-order approximate coupled cluster singles and doubles model CC2. *Chem. Phys. Lett.* **1995**, *243*, 409−418.
(42) Dunning, T. H., Jr.; Peterson, K. A.; Wilson, A. K. Gaussian basis sets for use in correlated molecular calculations. X. The atoms aluminum through argon revisited. *J. Chem. Phys.* **2001**, *114*, 9244−9253.
(43) Weigend, F.; Kohn, A.; Hattig, C. Efficient use of the correlation consistent basis sets in resolution of the identity MP2 calculations. *J. Chem. Phys.* **2002**, *116*, 3175−3183.
(44) Dunning, T. H., Jr. Gaussian basis sets for use in correlated molecular calculations. I. The atoms boron through neon and hydrogen. *J. Chem. Phys.* **1989**, *90*, 1007−1023.
(45) Kendall, R. A.; Dunning, T. H., Jr.; Harrison, R. J. Electron affinities of the first-row atoms revisited. Systematic basis sets and wave functions. *J. Chem. Phys.* **1992**, *96*, 6796−6806.
(46) Weigend, F.; Häser, M.; Patzelt, H.; Ahlrichs, R. RI-MP2: optimized auxiliary basis sets and demonstration of efficiency. *Chem. Phys. Lett.* **1998**, *294*, 143−152.
(47) Tsona, N. T.; Henschel, H.; Bork, N.; Loukonen, V.; Vehkamäki, H. Structures, hydration and electrical mobilities of bisulfate ion-sulfuric acid-ammonia/dimethylamine clusters - a computational study. *J. Phys. Chem. A* **2015**, *119* (37), 9670−9679.
(48) Wexler, A. Vapor pressure formulation for water in range 0 to 100 °C. A Revision. *J. Res. Natl. Bur. Stand., Sect. A* **1976**, *80A*, 775−785.
(49) Zurita-Gotor, M.; Rosner, D. E. Effective Diameters for Collisions of Fractal-like Aggregates:Recommendations for Improved Aerosol Coagulation Frequency Predictions. *J. Colloid Interface Sci.* **2002**, *255*, 10−26.
(50) Zhang, Y.; Li, S.; Yan, W.; Yao, Q.; Tse, S. D. Role of dipole-dipole interaction on enhancing Brownian coagulation of charge-neutral nanoparticles in the free molecular regime. *J. Chem. Phys.* **2011**, *134*, 084501.
(51) (a) DePalma, J. W.; Bzdek, B. R.; Ridge, D. P.; Johnston, M. V. Activation Barriers in the Growth of Molecular Clusters Derived from Sulfuric Acid and Ammonia. *J. Phys. Chem. A* **2014**, *118*, 11547−11554. (b) DePalma, J. W.; Bzdek, B. R.; Ridge, D. P.; Johnston, M. V. Correction to "Activation Barriers in the Growth of Molecular Clusters Derived From Sulfuric Acid and Ammonia". *J. Phys. Chem. A* **2015**, *119*, 931−932.

DOI: 10.1021/acs.jpca.5b11366
J. Phys. Chem. A 2016, 120, 1886−1896